Semiclassical spectrum using secular perturbation theory: the quartic oscillator

2000 J. Phys. A: Math. Gen. 33 93

(http://iopscience.iop.org/0305-4470/33/1/306)

J. Phys. A: Math. Gen. **33** (2000) 93–111. Printed in the UK PII: S0305-4470(00)03477-6

Semiclassical spectrum using secular perturbation theory: the quartic oscillator

Martin Müller and W D Heiss

Centre for Nonlinear Studies and Department of Physics, University of the Witwatersrand, PO Wits 2050, Johannesburg, South Africa

Received 14 April 1999, in final form 1 September 1999

Abstract. We analyse the quartic oscillator using the technique of removal of resonances in a region of parameter space where the system exhibits soft chaos. We obtain analytic expressions for all primary resonances and thus obtain a semiclassical spectrum. A criterion relating to overlapping resonances gives an estimate about the break down of the removal of resonance method.

1. Introduction

Single-particle motion in deformed mean fields has been traditionally studied in nuclear physics with considerable success [1]. The aspect of chaos was of minor importance at the time, since a nucleus is a comparatively small system, while, for the parameters used, the chaotic nature of the quantum spectrum manifests itself only at higher energies, that is beyond the region of interest for usual nuclear structure investigations. For larger systems, like electronic structures such as metallic clusters or quantum dots, the chaotic nature of deformed mean fields becomes a more important issue. Not only is an awareness of chaos of interest for technical reasons as in numerical work, but also new physical structures like shell formation are essentially influenced by the presence of chaotic motion [2].

There are a number of investigations concerning chaotic aspects for various types of deformed mean fields [3–5]. In the quoted studies the solution of particular potentials which are often used in phenomenological approaches has been obtained, but universal features have rarely been pointed out. What seems to be lacking is a systematic approach of quantum spectra associated with classical motion showing soft chaos. There is, of course, the trace formula where the relation between periodic orbits and the semiclassical spectrum is established. In the exhaustive book by Gutzwiller [9], the difficulty of the trace formula for soft chaos is discussed and attempts to tackle the problem are presented. In virtually all cases of interest the deformation of a single-particle potential can be considered as a perturbation of an integrable problem. It leads generically to a situation of soft chaos. This has been investigated in [7] where, however, the focus is upon the quantum states density. In [8], where individual energy levels have been calculated, it becomes clear that only a few, short periodic orbits are sufficient to adequately describe the quantum spectrum. In the range of validity of the approximation of this paper the accuracy achieved is similar to that in the above-quoted paper where an extension of the Berry–Tabor trace formula for integrable systems is used. Note that the authors emphasize the close relationship between the hyperbolic unstable and the elliptic stable periodic orbit of similar action: in fact, they form part of the same resonance.

0305-4470/00/010093+19$30.00

In this paper, we investigate this problem using as a case study the ubiquitous quartic oscillator. An essential point of this paper is the analytical tractability by which the basic principles and the step-by-step procedures are elucidated. The paper is motivated by our expectation that the methods developed here can be used, in principle, for a large class of similar problems; in fact, these expectations have been confirmed in certain special cases [4–6]. In general, in contrast to this paper, the appropriate transformations have to be performed numerically.

The quartic oscillator is a system that displays soft chaos. This means that appreciably large regions of stability exist in phase space. Moreover, only a finite, preferably small number of primary resonances (and possibly higher-order resonances) will be important for the corresponding quantum mechanical case. The simple nature of the quartic oscillator has evoked extensive studies, both for its classical [10–12], semiclassical [13–16], and its quantum mechanical aspects [17, 18]. We find analytic expressions for its resonances, and secular perturbation theory yields an explicit analytical form for each of the primary resonances.

Several mechanisms exist by which a system goes from integrability to global stochasticity. A stable resonance may undergo a bifurcation sequence, in which case a stable periodic orbit bifurcates until a dense set of trajectories associated with that resonance occupies a region of phase space. The semiclassical spectrum of these structures has been extensively studied [19, 20].

Secular perturbation theory [21] provides a general and transparent description of the mechanism by which global stochasticity emerges. In a separable, i.e. integrable, system the individual degrees of freedom are independent of each other. Once a perturbing term is added to the Hamiltonian, which destroys the integrability, regions of phase space lock onto the periodic orbits [22], in that the invariant tori are destroyed and replaced by many simultaneous resonances, also denoted as island chains. These resonant islands grow with the perturbation, but can in the generic case be well approximated by the pendulum Hamiltonian [21], as long as the perturbation is sufficiently small. Stochastic regions emerge around the separatrix and grow rapidly with the perturbation. To the extent that the stochastic regions of neighbouring resonances overlap, the system becomes globally stochastic. We use the onset of overlapping secondary resonances to estimate the size of the stochastic region near the separatrix.

Secular perturbation theory, as it is used here, is outlined by Lichtenberg and Lieberman [21]. The technique presented in this paper is entirely general, except for a straightforward adaptation used here because of a non-generic feature of the quartic oscillator, i.e. scaling. Section 2 is devoted to the theoretical background necessary to obtain the Hamiltonians near resonance. In section 3 we derive the semiclassical spectrum by repeatedly making use of EBK quantization of the approximately integrable Hamiltonian which describes the motion near the resonance. The resulting spectra are compared with the exact quantum mechanical results. The nature of our approximation and extensions to more general cases are discussed in section 4.

2. Classical mechanics and removal of resonances

The Hamilton function of the quartic oscillator is given by

$$H(p_1, p_2, q_1, q_2) = \frac{p_1^2 + p_2^2}{2m} + \alpha \frac{q_1^2 q_2^2}{2} + b q_1^4 + \frac{1}{b} q_2^4 \qquad b \geqslant 1$$

which is the most general form of the Hamiltonian for this particular problem [16]. When $\alpha = 0$ the Hamiltonian is integrable and has solutions in terms of elliptic integrals. Several other values of α exist for which this Hamiltonian is integrable [11]. As the Hamiltonian obeys

scaling [16], we need to solve the motion only at one energy. In the following, the Hamilton function is rewritten in terms of action and angle variables. If the actions are scaled by a factor γ, i.e. $J \to \gamma J$, the energy scales as

$$E \to \gamma^{\frac{4}{3}} E. \tag{1}$$

Action–angle variables are obtained by solving the Hamilton–Jacobi equation [23]. It yields a transformation to a coordinate system in which the Hamiltonian is independent of the coordinates, and only depends on integration constants. The actions are then simply functions of these constants. Finding the inverse of this map allows the integration constants to be written in terms of the actions, from which the transformation between action–angle coordinates and the original coordinate system is obtained [21].

Classical perturbation theory can be implemented using a coordinate system suitable for any 'adiabatic' constants. Action–angle coordinates are, however, well adapted to quantum mechanical problems.

For the unperturbed quartic oscillator ($\alpha = 0$) this procedure yields

$$\begin{aligned}
q_1(J_1, \Theta_1) &= \left(\frac{3J_1}{8\mathcal{K}}\right)^{\frac{1}{3}} \left(\frac{1}{2m}\right)^{\frac{1}{6}} \mathrm{sn}(4\mathcal{K}\Theta_1 - \mathcal{K}) \\
p_1(J_1, \Theta_1) &= \sqrt{2m \left(\frac{3J_1}{8\mathcal{K}}\right)^{\frac{4}{3}} \left(\frac{1}{2m}\right)^{\frac{2}{3}} b^{\frac{1}{3}} (1 - \mathrm{sn}^4(4\mathcal{K}\Theta_1 - \mathcal{K}))} \\
q_2(J_2, \Theta_2) &= \left(\frac{3J_2}{8\mathcal{K}}\right)^{\frac{1}{3}} \left(\frac{1}{2m}\right)^{\frac{1}{6}} \mathrm{sn}(4\mathcal{K}\Theta_2 - \mathcal{K}) \\
p_2(J_2, \Theta_2) &= \sqrt{2m \left(\frac{3J_2}{8\mathcal{K}}\right)^{\frac{4}{3}} \left(\frac{1}{2m}\right)^{\frac{2}{3}} \frac{1}{b^{\frac{1}{3}}} (1 - \mathrm{sn}^4(4\mathcal{K}\Theta_2 - \mathcal{K}))}
\end{aligned} \tag{2}$$

and

$$H_0(J_1, J_2) = \sqrt[3]{\left(\frac{3J_1}{8\mathcal{K}}\right)^4 \left(\frac{1}{2m}\right)^2 b} + \sqrt[3]{\left(\frac{3J_2}{8\mathcal{K}}\right)^4 \left(\frac{1}{2m}\right)^2 \frac{1}{b}}$$

where sn is the Jacobi elliptic function for $\kappa = -1$, and $\mathcal{K}$ is the complete elliptic integral of the first kind at $\kappa = -1$. Since there are several definitions for elliptic integrals and functions in use, we outline the definitions used in this paper in the appendix. From the previous equation we obtain for the winding number which is the ratio of the underlying frequencies

$$\frac{\omega_1}{\omega_2} = \frac{\left.\frac{\partial H_0}{\partial J_1}\right|_{J_2}}{\left.\frac{\partial H_0}{\partial J_2}\right|_{J_1}} = \sqrt[3]{b^2 \frac{J_1}{J_2}}. \tag{3}$$

The time dependence of Θ_1 and Θ_2 is $\omega_1 t + \Theta_{10}$ and $\omega_2 t + \Theta_{20}$, respectively. The full motion is thus mapped into $\Theta_1 \in [0, 1]$ and $\Theta_2 \in [0, 1]$. This defines the basic torus of the unperturbed problem. Closed orbits are obtained for commensurate frequencies. The resonance condition $\omega_1/\omega_2 = s/r$ with s and r integer, is manifestly a function of the actions.

The full Hamilton function ($\alpha \neq 0$) can now be represented in the unperturbed action–angle variables and is given by

$$\begin{aligned}
H(J_1, J_2, \Theta_1, \Theta_2) &= H_0(J_1, J_2) + \alpha H_1(J_1, J_2, \Theta_1, \Theta_2) \\
&= \left(\sqrt[3]{bJ_1^4} + \sqrt[3]{\frac{J_2^4}{b}}\right) \sqrt[3]{\left(\frac{3}{8\mathcal{K}}\right)^4 \left(\frac{1}{2m}\right)^2}
\end{aligned}$$

$$+\frac{\alpha}{2}\sqrt[3]{\frac{(9J_1J_2)^2}{(8\mathcal{K})^4(2m)^2}}\,\mathrm{sn}^2(4\mathcal{K}\Theta_1-\mathcal{K})\,\mathrm{sn}^2(4\mathcal{K}\Theta_2-\mathcal{K}). \tag{4}$$

We expand $H_1(J_1, J_2, \Theta_1, \Theta_2)$ as a Fourier series using the Fourier expansion [24] for sn, namely,

$$H_1(J_1, J_2, \Theta_1, \Theta_2) = \sum_{l,m} H_{l,m}(J_1, J_2)\exp(2\pi\mathrm{i}\{l\Theta_1 + m\Theta_2\})$$

where

$$H_{l,m}(J_1, J_2) = \frac{1}{2}\sqrt[3]{\frac{(9J_1J_2)^2}{(8\mathcal{K})^4(2m)^2}}\begin{cases} 0 & l, m \text{ odd} \\ \left(\dfrac{\mathcal{E}}{\mathcal{K}}-1\right)^2 & l = m = 0 \\ \left(\dfrac{\mathcal{E}}{\mathcal{K}}-1\right)\dfrac{\pi^2}{\mathcal{K}^2}\dfrac{\frac{m}{2}}{2\sinh\left(\frac{m\pi}{2}\right)} & l = 0, m \text{ even} \\ \left(\dfrac{\mathcal{E}}{\mathcal{K}}-1\right)\dfrac{\pi^2}{\mathcal{K}^2}\dfrac{\frac{l}{2}}{2\sinh\left(\frac{l\pi}{2}\right)} & l \text{ even}, m = 0 \\ \dfrac{\pi^4}{\mathcal{K}^4}\dfrac{\frac{lm}{4}}{4\sinh\left(\frac{l\pi}{2}\right)\sinh\left(\frac{m\pi}{2}\right)} & \text{otherwise.} \end{cases}$$

Here $\mathcal{E}$ is the complete elliptic integral of the second kind ($\kappa = -1$). Below we exploit the fact that the coefficients of this series fall off exponentially with increasing l and m.

The removal of resonance method is based upon a judiciously chosen series of suitable canonical transformations. The underlying principle of such transformations is outlined in figure 1. Action–angle coordinates of the unperturbed system are a convenient set of adiabatic variables to approximate the motion everywhere except near the periodic orbits. There the topology of the trajectories is different from the one of the integrable system, which requires another suitable transformation to be made.

The first transformation is indicated by the transition from figure 1(*a*) to (*b*). In this first step the Hamiltonian is rewritten in terms of action–angle variables of the unperturbed quartic oscillator. Both diagrams represent a Poincaré surface of section. As we focus our attention upon situations which are characterized by soft chaos, the Poincaré surface of section resembles an unperturbed situation. There are trajectories which lie on a torus which is only slightly distorted from that of the unperturbed problem, as is illustrated in figure 1(*a*) by dashed curves. In action–angle variables these trajectories have nearly constant action. This is illustrated in figure 1(*b*) (dashed curves), where phase space is essentially described by the unperturbed torus except for the vicinity of a resonance.

In the unperturbed problem where the winding numbers are fixed solely by the constant actions, a continuous set of periodic orbits exists for a given winding number, since arbitrary values of the angles satisfying the resonance condition yield periodic orbits. This trivial degeneracy is removed by the switching on of the perturbation. Generically, one stable periodic orbit or fixed point remains. Details are displayed in figure 2. The dashed line i in figure 2(*a*) and the central point in figure 2(*b*) is the stable orbit. It is associated with an unstable periodic orbit (iii in figure 2(*a*)). The unstable periodic orbit is indicated by small circles in figure 2(*b*) and the separatrix related to it by the symbol iii. For clarity of illustration the separatrix of the corresponding pendulum Hamiltonian is drawn rather than that of the full problem, which would be difficult to display (it is a homo-clinic tangle: see, e.g. [9]). Near the stable periodic orbit, a swarm of trajectories becomes attached to it by phase locking. A wavy curve in the Θ_1–Θ_2 plane (solid curve ii in figures 2(*a*) and (*b*)) characterizes their typical behaviour. These new tori which are associated with the resonance, i.e. the stable orbit, bring about the break

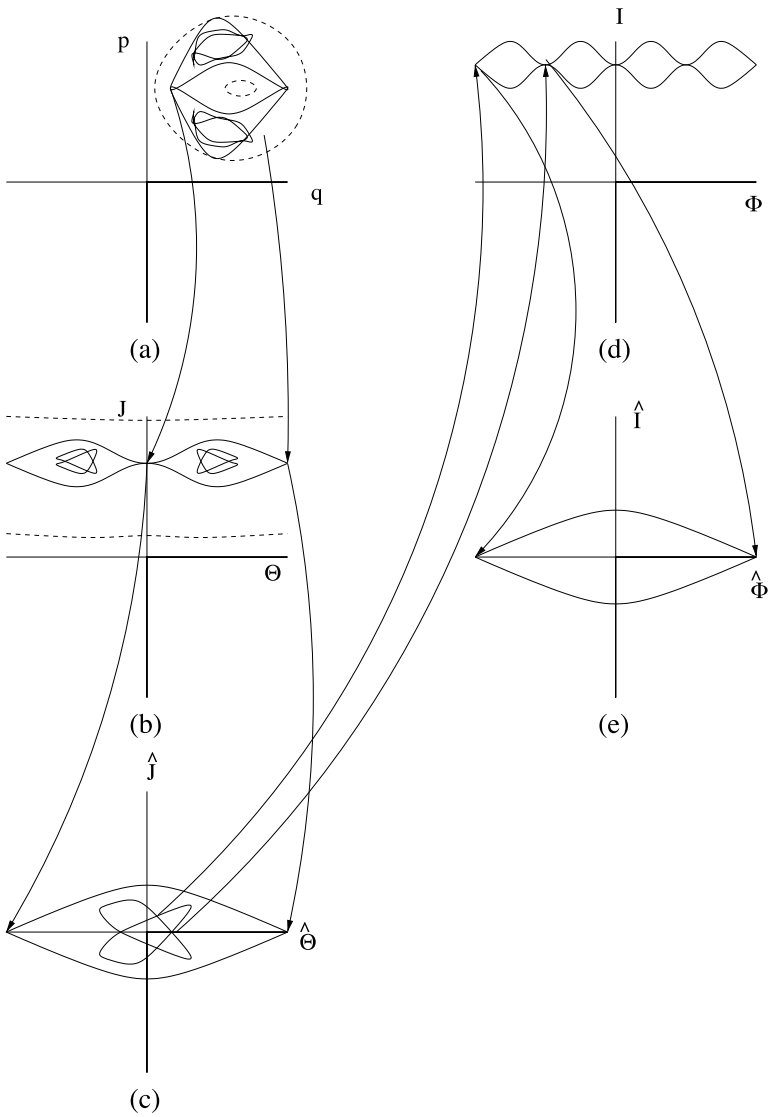

Figure 1. Schematic diagram illustrating the successive transformation for the removal of primary and higher-order resonances.

up of the original torus [3] which is defined by the unperturbed problem. Trajectories with an action that is sufficiently distant from the resonance, so that they are not trapped by the resonance, move essentially on the torus of the unperturbed system (iv in figures 2(*a*) and (*b*)). They are well approximated by a Hamiltonian which is obtained by averaging over the angles.

The second step illustrates the transformation to a coordinate system that is co-moving with the resonance, as is represented in the transition from figure 1(*b*) to (*c*). The motion near the resonance is approximated well by that of a pendulum as long as the perturbation is not too large. However, $\hat{J}$ is not constant but time dependent due to the angle-dependent terms in the perturbing potential H_1.

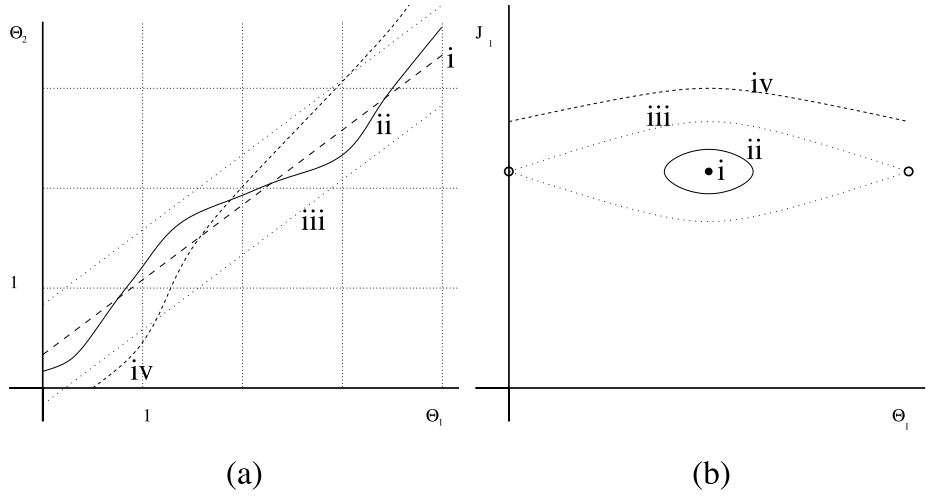

Figure 2. Illustration of various types of motion for the full problem. Trajectories are given in angle coordinates (*a*), and a fraction of phase space (surfaces of section) in action–angle coordinates (*b*). For further explanation see the text.

Although removing a resonance cannot approximate the homo-clinic tangle, the neighbourhood of the stable fixed point is to second order a harmonic oscillator and the unstable fixed point an inverted harmonic oscillator. As these fixed points are approximated by functions dependent on the 'adiabatic' actions, they will vary little with the perturbation. Thus the stability coefficients needed for the trace formula are adequately taken into account. Since the action of the pendulum is well described by a linear approximation, the motion inside the separatrix resembles a harmonic oscillator, while outside the separatrix it resembles an inverted oscillator. Any stable resonance with a region of stability too small to generate an energy level will thus behave as if it was an unstable periodic orbit in the trace formula. As we assume that the trace formula gives a good description of the chaotic region, we ignore this effect and concentrate on the region inside the separatrix.

Once we have made the pendulum approximation, we obtain an integrable Hamiltonian in a limited domain of phase space as an approximation. It can be expressed in its action–angle variables. The transformation is illustrated by the transformation from figure 1(*c*) to (*d*). The motion is perturbed by higher-order resonances between the effective pendulum frequency and the original resonance frequency. This is indicated by islands in figure 1(*d*). For each higher-order resonance, we can again transform to a coordinate system that is co-rotating with the resonance, as is illustrated by the transformation from figure 1(*d*) to (*e*).

Since the period of a pendulum increases near its separatrix, higher-order resonances emerge at an increasing rate. It can also be shown that the sizes of the separatrices of these new resonances grow rapidly near the original pendulum separatrix [21], where the sizes of the new resonances are again measured by the position of the separatrix of the integrable system approximating the motion near the periodic orbit. This combined effect creates the stochastic region. A reasonable criterion about the border line of the stochastic region surrounding the primary resonance is therefore the first overlap of higher resonances near the separatrix. More sophisticated techniques, such as those outlined in [21] or in [25] may yield a more precise delineation of the stochastic region, but the appeal of the present method lies in its conceptual simplicity when the interest is focused on the semiclassical spectrum.

In the following, we exemplify the procedure and consider a particular resonance with the winding number s/r. We follow the method outlined in [21] except that we choose the transformation which retains the periodicity in the interval [0 : 1] in the new coordinates. This choice, outlined in [9] makes no difference to the classical description, but simplifies the semiclassical calculations as shown below. The canonical transformation

$$\begin{aligned}\hat{J}_1 &= J_1\\ \hat{J}_2 &= r J_2 + s J_1\\ \hat{\Theta}_1 &= \Theta_1 - \frac{s}{r}\Theta_2\\ \hat{\Theta}_2 &= \frac{\Theta_2}{r}\end{aligned} \tag{5}$$

transforms to a frame where $\dot{\hat{\Theta}}_1 = \dot{\Theta}_1 - (s/r)\dot{\Theta}_2 = \omega_1(J_1, J_2) - (s/r)\omega_2(J_1, J_2)$ measures the deviation from the resonance. It is small near the resonance $\omega_1/\omega_2 = s/r$, and vanishes at the resonance. Averaging over the fast angle, $\hat{\Theta}_2$, yields

$$\bar{H} = \bar{H}_0(\hat{\boldsymbol{J}}) + \alpha \bar{H}_1(\hat{\boldsymbol{J}}, \hat{\Theta}_1)$$

where

$$\bar{H}_1 = \langle \hat{H}_1(\hat{\boldsymbol{J}}, \hat{\boldsymbol{\Theta}})\rangle_{\Theta_2} = \sum_{p=0}^{\infty} H_{-pr,ps}(\hat{\boldsymbol{J}})\mathrm{e}^{-2\pi \mathrm{i} p\hat{\Theta}_1}.$$

This approximate Hamiltonian is expected to be good near the resonance. Since it is independent of $\hat{\Theta}_2$, the action $\hat{J}_2 = J_2 + (s/r)J_1$ is a constant of motion. As the higher-order terms in the Fourier expansion fall off exponentially, we ignore the terms with $|p| > 1$ in the series. The approximate Hamiltonian describing the motion near the resonance is then given by

$$\begin{aligned}\bar{H}_{r,s} = \sqrt[3]{\left(\frac{3}{8\mathcal{K}}\right)^4\left(\frac{1}{2m}\right)^2}\Bigg(\sqrt[3]{b\hat{J}_1^4} + \sqrt[3]{\frac{(\hat{J}_2/r - (s/r)\hat{J}_1)^4}{b}} + \frac{\alpha}{2}\sqrt[3]{(\hat{J}_1)^2(\hat{J}_2/r - (s/r)\hat{J}_1)^2}\\ \times\left\{\left(\frac{\mathcal{E}}{\mathcal{K}} - 1\right)^2 + \frac{\pi^4}{8\mathcal{K}^4}\frac{rs}{\sinh\frac{r\pi}{2}\sinh\frac{s\pi}{2}}\cos 2\pi\hat{\Theta}_1\right\}\Bigg).\end{aligned} \tag{6}$$

The illustration in figure 3 for the perturbation $\alpha = 0.1$ and $\alpha = 1$ confirms the good quality of the description of the exact situation.

For increasing α the two main resonances, i.e. those with dominant Fourier components, begin to overlap. It occurs when two independent resonances, after they have been removed, share the same region of phase space.

Comparing the Poincaré surface of section of the full Hamiltonian in figure 3(*c*). with the section where the resonance has been removed, figure 3(*d*), the effect of one resonance on the other can clearly be seen. The approximate Hamiltonian cannot reflect this, as the approximation contains no information about other resonances.

We now transform to the action–angle coordinates of the Hamiltonian near the resonance (denoted by I and Φ in figure 1(*d*)). Since equation (6) is independent of Θ_2, $I_2 = \hat{J}_2$ is already in the correct form. Solving equation (6) for $\cos\hat{\Theta}_1$ we can evaluate explicitly

$$I_1 = \oint \hat{J}_1\,\mathrm{d}\hat{\Theta}_1. \tag{7}$$

In figure 4(*a*), $\cos\hat{\Theta}_1$ is plotted as a function of $\hat{J}_1$ for various values of $\hat{J}_2$. The corresponding plot for $\hat{\Theta}_1$ is displayed in figure 4(*b*). The periodic orbit in figure 4(*a*) corresponds to the point where the vertex of the parabola-type curves coincides with $\cos\hat{\Theta}_1 = -1$ (diamond), while

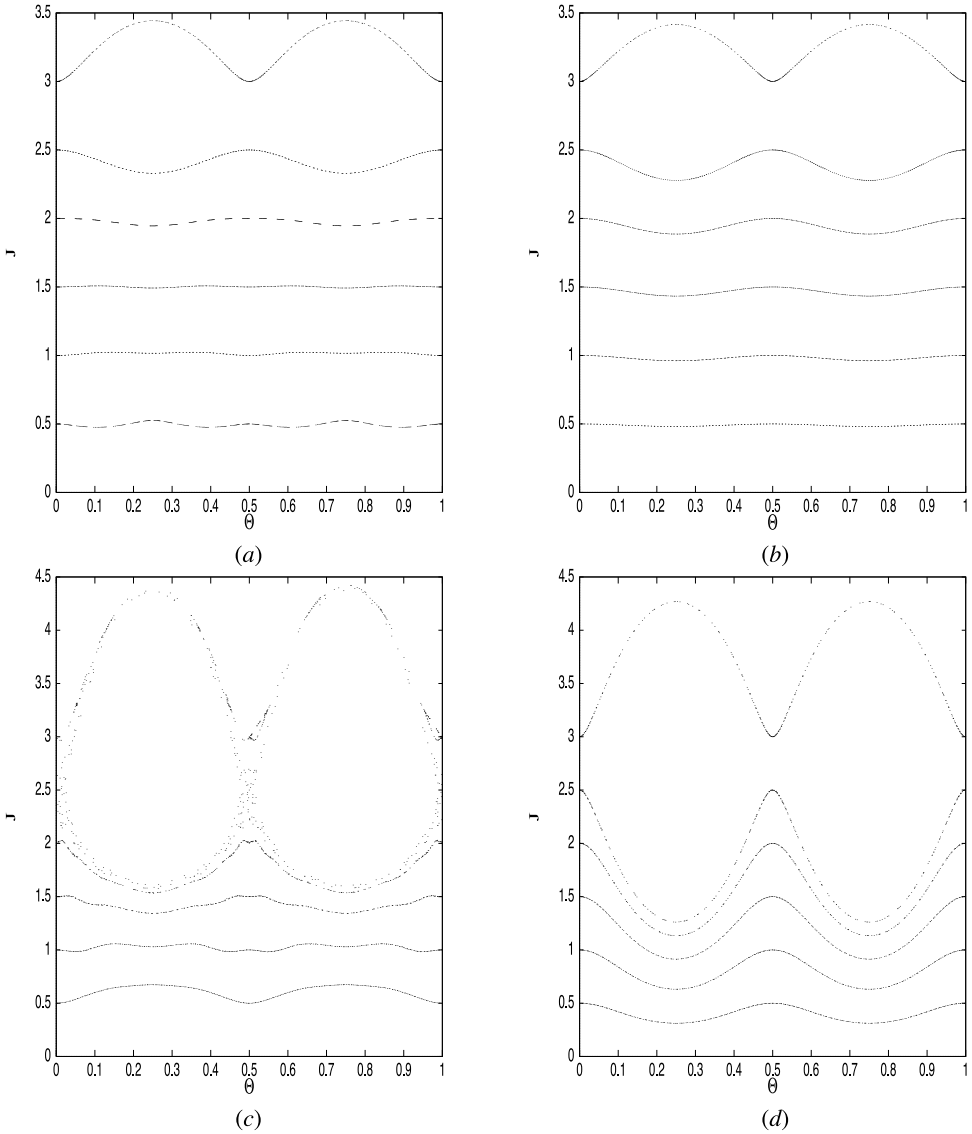

Figure 3. Poincaré surface of section at $E = 1$ for the quartic oscillator for $\alpha = 0.1$ (*a*) and $\alpha = 1$ (*c*). The Poincaré surface of section of the Hamiltonian taking into account the principle resonance, $r = s = 2$ is shown for $\alpha = 0.1$ (*b*) and $\alpha = 1$ (*d*).

the separatrix is given by the curve whose vertex coincides with $\cos\hat{\Theta}_1 = 1$ (solid curve). The dependence on $\hat{J}_2$ is nearly linear within the region between the two values for $\cos\hat{\Theta}_1$.

To evaluate the integral we make a simplifying approximation. We consider only terms up to second order in $\hat{J}_1$ and first order in $\hat{J}_2$ in a Taylor expansion of $\cos\hat{\Theta}_1$. In this way we obtain the pendulum equation (see the appendix), namely,

$$\hat{J}_2 - \hat{J}_{2\mathrm{res}} = \frac{G}{2}(\hat{J}_1 - \hat{J}_{1\mathrm{res}})^2 - F\cos(2\pi\hat{\Theta}_1)$$

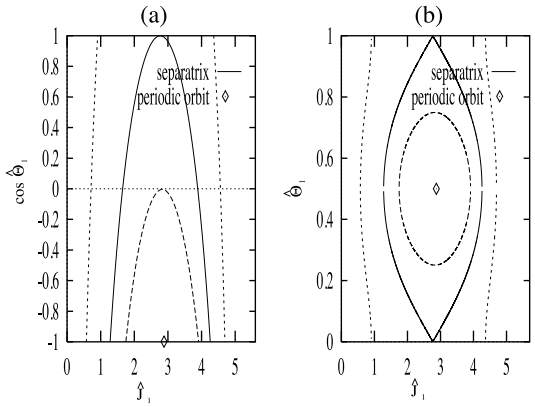

Figure 4. (*a*) Plot of $\cos 2\pi\hat{\Theta}_1$ as a function of $\hat{J}_1$ and (*b*) $\hat{\Theta}_1$ as a function of $\hat{J}_1$ for various $\hat{J}_2$ at $\alpha = 1$.

with

$$\frac{1}{F} = -\left.\frac{\partial \cos 2\pi\hat{\Theta}_1}{\partial \hat{J}_2}\right|_{\text{res}}$$
$$\frac{G}{F} = \left.\frac{\partial^2 \cos 2\pi\hat{\Theta}_1}{\partial \hat{J}_1^2}\right|_{\text{res}}.$$

Note that we use here the same symbols F (and G) even though they denote an action (an inverse action) while they refer to an energy (an inverse moment of inertia) in the appendix.

From figure 4 the stable or unstable fixed points occur at $\cos\hat{\Theta}_1 = \pm 1$. Since the choice depends on the sign of F/G, choosing the stable fixed point leads to a discontinuous spectrum at $\alpha = 0$. To obtain a smooth dependence of F and G and thus the spectrum over the entire resonance, we expand around the point $(\Theta_{1\text{res}}, J_{1\text{res}})$ which is determined by the two conditions

$$\frac{\partial \cos 2\pi\hat{\Theta}_1}{\partial \hat{J}_1} = 0$$
$$\cos 2\pi\hat{\Theta}_1 = 0.$$

The separatrix is given by

$$\hat{J}_2 = \hat{J}_{2\text{res}} \pm F. \tag{8}$$

Making use of the action of a pendulum, the second action equation (7) is given inside the separatrix by

$$I_1' = I_1(E=1) = 8\sqrt{\frac{2(\hat{J}_2 - \hat{J}_{2\text{res}} + F)}{G}}$$
$$\times \left(\sqrt{\frac{\hat{J}_2 - \hat{J}_{2\text{res}} + F}{2F}} - \sqrt{\frac{2F}{\hat{J}_2 - \hat{J}_{2\text{res}} + F}}\right) \mathcal{K}\left(\frac{\hat{J}_2 - \hat{J}_{2\text{res}} + F}{2F}\right)$$
$$+\sqrt{\frac{2F}{\hat{J}_2 - \hat{J}_{2\text{res}} + F}}\,\mathcal{E}\left(\frac{\hat{J}_2 - \hat{J}_{2\text{res}} + F}{2F}\right). \tag{9}$$

This expression is used below, when the effect of a primary resonance upon the quantum spectrum is calculated.

2.1. Higher-order removal of resonance—demarcation of the stochastic region

To obtain an intuitive feeling for the breakdown of the validity of the first-order resonance we briefly outline the effect of higher-order resonances. However, the method presented here is not necessarily satisfactory in qualitative terms and is therefore not used for further improvement of the quantum spectrum. It gives an understanding of the limitations of an analytic perturbative approach of this kind.

The approximate Hamiltonian near resonance, denoted by K_0, is again integrable, with actions I_1 and I_2. The terms left out in removing the primary resonance can be re-introduced as a perturbation on the new Hamiltonian. The new frequencies are

$$\hat{\omega}_1 = \frac{\partial K_0}{\partial I_1}$$
$$\hat{\omega}_2 = \frac{\partial K_0}{\partial I_2} = \frac{\omega_2}{r}$$

where $\hat{\omega}_1$ is given approximately by the pendulum Hamiltonian. We consider for the higher-order resonance

$$\frac{\hat{\omega}_2}{\hat{\omega}_1} = \frac{p}{q}.$$

Following Lichtenberg and Lieberman [21] section 2.6, the Hamiltonian near the higher-order resonance is given by

$$H_{r,s,p,q} = G'(\Delta I_1)^2 + \mathcal{J}_p\left(\sqrt{\frac{I_{10}}{\pi}\sqrt{\frac{G}{F}}}\right) H_{r,s-q} \cos 2\pi\phi$$

where $\mathcal{J}_p(x)$ is the Bessel function of order p, I_{10} is I_1 evaluated at the resonance and we use the approximation

$$G' \approx \frac{\partial \hat{\omega}_1}{\partial I_1}$$

as $\partial\hat{\omega}_1/\partial I_1$ is expected to be the dominant contribution of $\partial^2 K_0/\partial \hat{I}_1^2$. Solving for the variation in ΔI_1 at the separatrix, we have an estimate of the size of the resonance in I_1:

$$\Delta I \approx \sqrt{\frac{H_{r,s-q}\mathcal{J}_p\left(\sqrt{\frac{I_{10}}{\pi}\sqrt{\frac{G}{F}}}\right)}{G'}}.$$

The behaviour of higher-order resonances is outlined in figure 5. As the separatrix is approached more and more resonances exist. The island size also grows rapidly as a function of I_1. Thus near resonance many islands will overlap. The first overlap of two neighbouring islands is a good indication of the outermost intact KAM surface. For the quartic oscillator even for $\alpha \approx 1$, the value of the perturbation where we the pendulum equation becomes inadequate, more than 90% of phase space (when measured as the fraction of phase space that is regular in terms of I_1) is still regular.

3. The semiclassical spectrum

For an integrable system the quantum spectrum is obtained by the EBK quantization. This is obvious for $\alpha = 0$. If α is nonzero, the system is no longer integrable, yet it is well approximated by an adiabatic Hamiltonian which is obtained by taking the mean over the

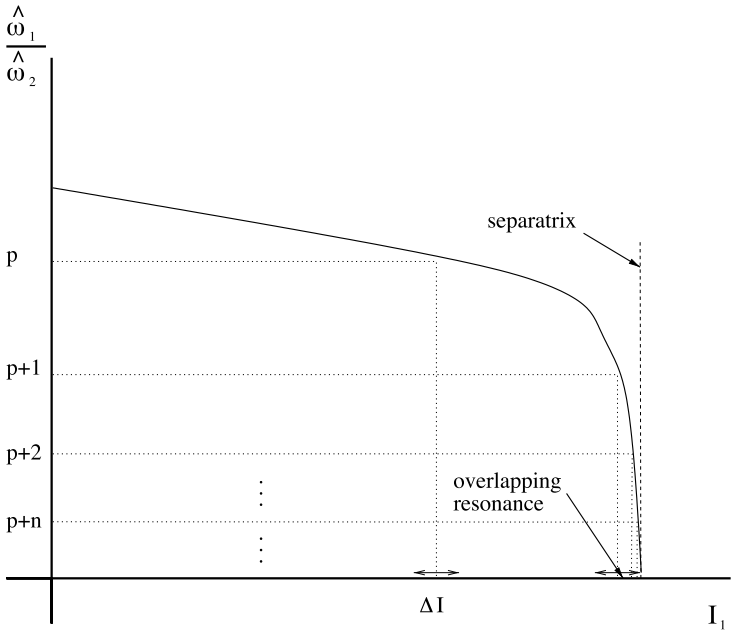

Figure 5. The behaviour of higher-order resonances.

angles, if α is not too large. The approximation is good as long as the periodic orbits do not trap a large part of phase space. In fact, any structure in phase space smaller than $\overline{h}$ will not feature in the quantum spectrum. In turn, the neighbourhood of each orbit which traps a larger region can be treated using the approximate Hamiltonian as described in the previous section. The essential point is that the new, locally approximate Hamiltonian is integrable and can therefore also be quantized using EBK quantization.

This can lead in general to multiple representations of phase space. We therefore should find an estimate as to which Hamiltonian to use in order to obtain the semiclassical spectrum. As long as the perturbation is small, and the stochastic regions as well as the regions dominated by the resonances are small, it is straightforward to choose the best approximation. Once the resonances are large and begin to overlap, several sets of quantum numbers may describe the same region of phase space. In such a case, a general criterion for the best choice does not seem to be at hand.

3.1. The semiclassical spectrum without resonances

When the perturbation is small, the motion can be approximated by deforming the exact tori. This is obtained by ignoring the finer structure of the topology of trajectories near the resonances. An averaging over the angle-dependent part of the full Hamiltonian thus results in an approximate potential which we call the adiabatic potential.

Once we have obtained the integrable adiabatic Hamiltonian, we obtain a semiclassical spectrum via the procedure described by EKB. This procedure requires

$$\oint p \, \mathrm{d}q = h\left(n + \frac{\beta_i}{4}\right)$$

where β_i is the Maslov index. It increases by unity each time the periodic orbit makes a soft collision off a caustic, which is in the present case the edge of the potential.

For the quartic oscillator (and for the harmonic oscillator) the Maslov index is two for each degree of freedom. Thus the quantization condition reads

$$\oint p_1 \mathrm{d}q_1 = 2\pi\hbar(n + \tfrac{1}{2})$$
$$\oint p_2 \mathrm{d}q_2 = 2\pi\hbar(m + \tfrac{1}{2})$$

or

$$J_1 = 2\pi\hbar(n + \tfrac{1}{2})$$
$$J_2 = 2\pi\hbar(m + \tfrac{1}{2}).$$

When this is inserted into the adiabatic Hamiltonian, the semiclassical energy eigenvalues $E_{m,n}$ are obtained by averaging equation (4) over Θ_1 and Θ_2. This amounts to taking only the constant term in the Fourier expansion and reads

$$E_{n,m}(\alpha) = \left(\sqrt[3]{b\left(2\pi\hbar\left(n+\frac{1}{2}\right)\right)^4} + \sqrt[3]{\frac{(2\pi\hbar(m+\frac{1}{2}))^4}{b}}\right)\sqrt[3]{\left(\frac{3}{8\mathcal{K}(-1)}\right)^4\left(\frac{1}{2m}\right)^2}$$
$$+\frac{\alpha}{2}\sqrt[3]{\frac{((6\pi\hbar)^2(n+\frac{1}{2})(m+\frac{1}{2}))^2}{(8\mathcal{K}(-1))^4(2m)^2}} \times \left(\frac{\mathcal{E}(-1)}{\mathcal{K}(-1)} - 1\right)^2. \tag{10}$$

The spectrum is plotted in figure 6. Obviously no level repulsions can occur, the approximate spectrum can have only genuine level crossings. Around $\alpha = 0$ the spectrum is virtually exact except for the lowest levels, where the approximation involving the Maslov indices is unreliable (recall that even at $\alpha = 0$ the spectrum is only a semiclassical approximation). Globally, the spectrum does present an astoundingly fair approximation towards the exact spectrum.

3.2. The semiclassical spectrum near resonance

When the perturbation increases, larger regions of phase space begin to phase lock onto the periodic orbits of the system. The trajectories are no longer straight lines in angle coordinates, but begin to oscillate about fixed points. In other words, one particular orbit among the unperturbed set becomes the stable centre of trajectories in its vicinity, which phase lock onto it. The actual perturbation determines which particular orbit is selected.

Following the discussion in section 2, secular perturbation theory approximates the motion near the resonance by an integrable Hamiltonian. As this Hamiltonian is well approximated by a pendulum Hamiltonian, the separatrix of the pendulum gives a good measure of how much of phase space is dominated by the resonance. As outlined in the appendix, and illustrated in figure 7, the motion is described by a vibration about the fixed point for energies between $-F$ and F. Thus, in terms of $\hat{J}_2$, the region dominated by the resonance is given by

$$\hat{J}_{2\mathrm{res}} - F < \hat{J}_2 < \hat{J}_{2\mathrm{res}} + F.$$

We rewrite this condition in terms of the original variables using equation (5) to obtain the separatrix condition

$$J_2 = \hat{J}_{2\mathrm{separatrix}} - \frac{s}{r}J_1.$$

The intersection points of the energy and separatrix conditions (figure 7) demarcate the region dominated by the resonance at a given energy ($E = 1$). From scaling the region in J_1 and J_2 can then be delineated.

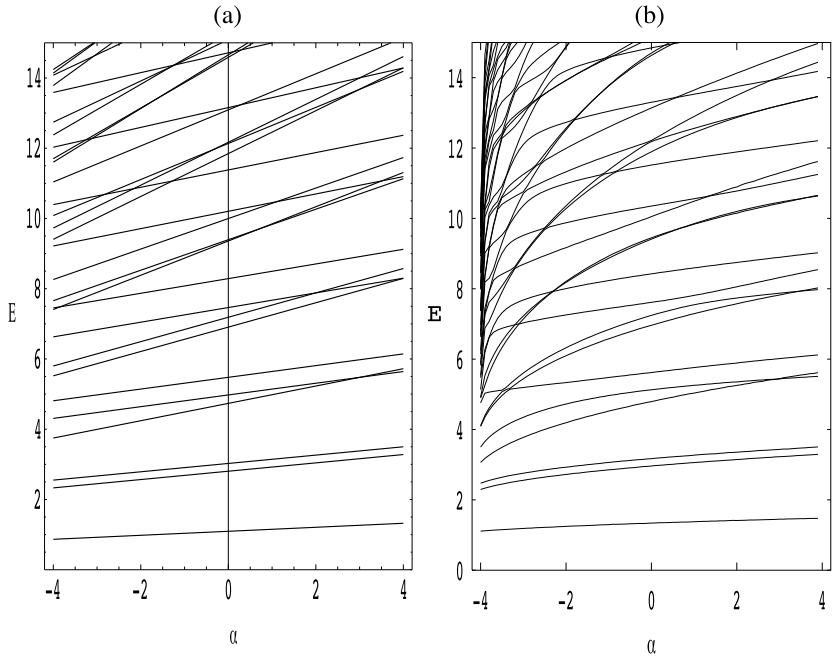

Figure 6. (*a*) Graph of E_{mn} neglecting the effect of resonances for $b = 1.2$ and (*b*) the quantum mechanical spectrum, where $\overline{h} = 1$ and $m = 1$.

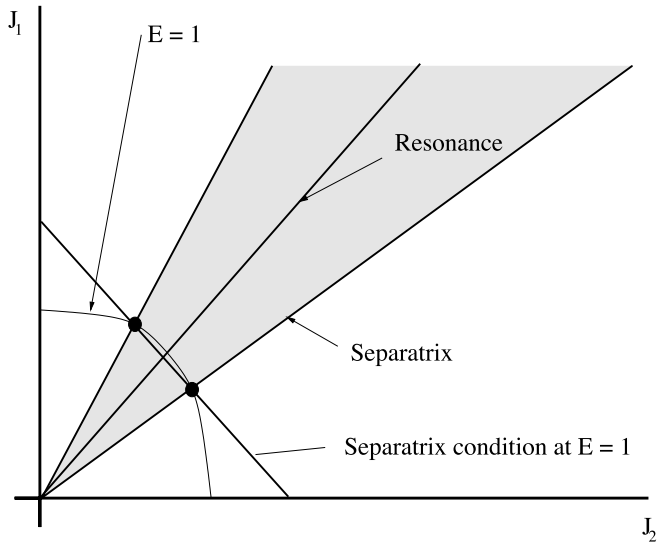

Figure 7. Diagram illustrating the region of phase space dominated by a particular resonance.

Inside the resonance the values of J_1 and J_2 are well approximated by the integrable Hamiltonian of equation (6). The old angles in terms of the new angles $(\hat{\Theta}_1, \hat{\Theta}_2)$ are given by

$$\Theta_1 = \hat{\Theta}_1 + s\hat{\Theta}_2$$
$$\Theta_2 = r\hat{\Theta}_2.$$

EBK quantization requires that the actions around each topologically distinct closed curve, C_1 and C_2 on the torus, be a multiple of Planck's constant. In Θ_1 and Θ_2 coordinates, this occurs whenever Θ_1 or Θ_2 change by unity. Thus C_1 and C_2 are associated with Θ_1 and Θ_2 changing respectively by unity. The equation above shows that when $\hat{\Theta}_1$ changes by unity, only C_1 is traversed. Changing $\hat{\Theta}_2$ by unity traverses C_1 r times and C_2 s times.

The Hamiltonian near resonance has the actions

$$I_1 = \oint \mathrm{d}\hat{\Theta}_1 \, \hat{J}_1$$
$$I_2 = \oint \mathrm{d}\hat{\Theta}_2 \, \hat{J}_2$$

and hence the semiclassical quantization conditions:

$$I_1 = h\left(m' + \frac{\nu_1}{4}\right)$$
$$I_2 = h\left((r+s)n' + \frac{\nu_2}{4}\right)$$

where $\nu_2 = 2(r+s)$ is the Maslov index of the primitive periodic orbit (as the particle makes $2r$ collisions with the caustic in the q_1 direction and $2s$ in the q_2 direction) and $\nu_1 = 2$ is due to the soft collision of the pendulum boundary.

The full spectrum which is brought about by the contribution of the resonance is obtained by exploiting scaling. Since I_1 and I_2 are actions, they scale linearly. We use the quantum condition, namely,

$$\frac{I_1}{I_2} = \frac{I_1'}{I_2'} = \frac{m' + \frac{1}{2}}{n' + \frac{\nu_2}{4}}$$

where $I_1' = I_1(E=1)$ and $I_2' = I_2(E=1)$. Inserting equation (9) for I_1' yields

$$\frac{m' + \frac{\nu_1}{4}}{n' + \frac{\nu_2}{4}} = \frac{8}{I_2'}\sqrt{\frac{2(\hat{I}_2 - \hat{J}_{2\mathrm{res}} + F)}{G}} \times \left[\left(\sqrt{\frac{I_2' - \hat{J}_{2\mathrm{res}} + F}{2F}} - \sqrt{\frac{2F}{I_2' - \hat{J}_{2\mathrm{res}} + F}}\right)\mathcal{K}\left(\frac{I_2' - \hat{J}_{2\mathrm{res}} + F}{2F}\right) + \sqrt{\frac{2F}{I_2' - \hat{J}_{2\mathrm{res}} + F}}\,\mathcal{E}\left(\frac{I_2' - \hat{J}_{2\mathrm{res}} + F}{2F}\right)\right]$$

for $|\hat{J} - \hat{J}_{\mathrm{res}}| < |F|$. This equation can be solved for I_2'. Using I_2' at $E = 1$ and scaling it to the required value $I_2 = n' + \nu_2/4$, gives the spectrum

$$E_{m',n'} = \left(\frac{n' + \nu_2/4}{I_2'}\right)^{\frac{4}{3}}.$$

Recall that I_2' is a function of the quotient $(m' + \frac{1}{2})/(n' + \nu_2/4)$.

The quality of this approximation is displayed in figure 8. Note that the linear dependence on α no longer prevails in contrast to figure 6. The diagram displays energy levels expected to be the worst, as the approximation of a linear edge for the potential fails for the low-lying energy levels and are therefore incorrectly modelled by the Maslov index. It is true that the correction obtained from the resonance is small, yet it represents the correct trend of the quantum spectrum. Since the pendulum equation is expected to be correct only near the integrable system, higher-order terms in α (for $\alpha < 0$) are expected to improve the approximation. However, one

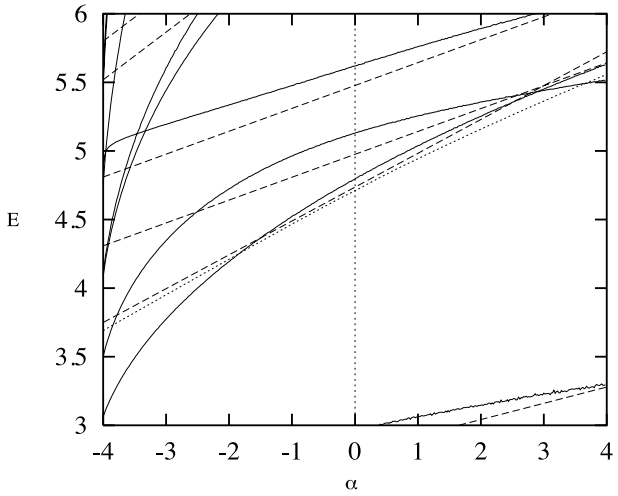

Figure 8. The solid curves are the quantum spectrum, dashed lines are the adiabatic spectrum E_{mn} and the dotted curve is $E_{m'n'}$ of the principal resonance $r = s = 2$.

cannot hope that the approximate integrable system obtained by the removal of resonance technique would give the correct spectrum far into the chaotic region. The apparent poor performance of the spectrum displayed in figure 8 near the integrable case is due to the fact that the resonance does not occupy sufficient phase space so as to capture an energy level in the range $\alpha \in [-0.1, 0.1]$. The loss of intensity from the adiabatic spectrum $E_{m,n}$ to the spectrum of the resonance $E_{m',n'}$ in regions of phase space, where both integrable systems approximately describe the same part of that phase space, is not taken into account in this paper. Neglecting this loss of intensity gives a spectrum that is discontinous. In the limit $\alpha \to 0$, no resonance can trap any energy levels, and the integrable semiclassical spectrum prevails.

4. Conclusion

It has been accepted wisdom since the early days of quantum mechanics, that the essential coordinates for the quantum mechanical understanding of a classical system are action–angle coordinates. Yet, this important insight has rarely been put to work. Obviously, expressing a phenomenological potential in spatial coordinates is intuitively more appealing, and rewriting a Hamilton function in action–angle coordinates is, in general, an arduous task and usually not amenable to closed analytic expressions. In this paper we have attempted to make the point that a perturbative approach in terms of action–angle variables does yield a quantum mechanical spectrum from a classical analysis. The particular choice of the quartic oscillator is made as it permits analytic elaboration in terms of higher transcendental functions, which renders the principle and the treatment transparent and illustrative.

The approach is perturbative in nature. The procedure for refinement is well defined in principle and the limitations are delineated. The treatment of perturbation is classical and is totally different from the treatment traditionally used in quantum mechanics. There one would use, to lowest order, the corrections $\Delta E_{m,n} = \langle n, m|H_1|n, m\rangle$. While it is obvious that this traditional perturbative approach is bound to fail in a chaotic system except for very small values of α (which is not within our interest), our procedure uses the appropriate procedure for such cases, which is the removal of resonance method. Therefore, even in the zeroth-

order approximation, which is the averaged Hamiltonian, the levels are assigned quantum numbers that are different from the ones that would emerge in a traditional quantum mechanical perturbative approach. The new sets of quantum numbers come about in a natural way. The assignments take into account the important resonances and are modified as indicated. As a consequence, while the levels for $\alpha = 0$ do not coincide with the actual unperturbed levels, they are superior to the traditional perturbative approach for α sufficiently different from zero.

The discrepancy between the exponential growth of the number of classical periodic orbits and the power law of the number of quantum levels is resolved in a natural way: separatrices associated with resonances which cover an area of phase space smaller than $\overline{h}$ simply do not feature in the quantum spectrum. In other words, only those unstable orbits, associated with a stable orbit having a stability region covering a sufficiently large area of phase space, give rise to a quantum level. Note that unstable orbits do not directly lead to an energy level, only a stable periodic orbit does (see section 17.6 of [9]). Consequently, an appreciably limited number of resonances contribute to the quantum spectrum while the fast growing number of insignificant resonances remains unnoticed in the quantum spectrum. We believe that this view adds to the interpretation of the trace formula in a system showing soft chaos. We note in passing that, due to scaling, a resonance produces an infinite set of quantum numbers for the quartic oscillator; this is in general not the case.

Work is in progress where the same method is used for the deformed Woods–Saxon potential which is likewise a problem exhibiting soft chaos [2]. There, the corresponding Fourier transforms can be carried out only numerically, but this is no longer a basic problem owing to modern computers. The interesting aspect is the dependence of the potential on the actions (angles) specific to the Woods–Saxon potential due to its flat bottom and steeper walls. We believe that, once one has become accustomed to 'view' a potential in its action dependence rather than in its spatial form, a crucial step has been made towards the quantum mechanical analogy of a classical motion in a potential that exhibits soft chaos. Such change of emphasis is expected to be helpful in interpreting observed spectra of mesoscopic systems like quantum dots or metallic clusters as in these, owing to the larger particle number, the signature of soft chaos begins to have an impact upon the quantum spectrum.

Appendix. Miscellaneous forms and definitions

The Hamiltonian of the pendulum is given by

$$H(p,q) = \frac{G}{2}p^2 - F\cos(q)$$

where the terms for a pendulum in a gravitational field have the meaning

$$G = \frac{1}{ml^2}$$
$$F = mgl$$

with g being the acceleration due to gravity and m the mass of the pendulum assumed to be concentrated at the end of the massless rod of length l. The canonical coordinates p and q are the angular momentum and angle, respectively. The motion can be parametrized by the equation for the momentum, namely,

$$p = \sqrt{\frac{2(E + F\cos q)}{G}}.$$

A.1. The action of the pendulum

The action for the pendulum is given by the integral of the momentum over one cycle, which leads to

$$J = \oint \mathrm{d}q \sqrt{\frac{2(E + F\cos(q))}{G}}$$

which is given by

$$J = 8\sqrt{\frac{2(E+F)}{G}} \begin{cases} \mathcal{E}\left(\dfrac{2F}{E+F}\right) & \text{for} \quad E > F \\ \left(\sqrt{\dfrac{E+F}{2F}} + \sqrt{\dfrac{2F}{E+F}}\right)\mathcal{K}\left(\dfrac{E+F}{2F}\right) & \\ \quad + \sqrt{\dfrac{2F}{E+F}}\,\mathcal{E}\left(\dfrac{E+F}{2F}\right) & \text{for} \quad E < F \end{cases}$$

where $\mathcal{E}(\kappa)$ is the complete elliptic integral of the second kind and $\mathcal{K}(\kappa)$ is the complete elliptic integral of the first kind. We obtain the period frequency

$$\omega = \frac{1}{\frac{4}{\sqrt{2GE}} \int_0^{q_{\max}} \frac{\mathrm{d}q}{\sqrt{1+\frac{F}{E}\cos q}}}$$

which gives the time period

$$T = 8\sqrt{\frac{1}{2Gg(E+F)}} \begin{cases} \mathcal{K}\left(\dfrac{2F}{E+F}\right) & \text{for} \quad E > F \\ \sqrt{\dfrac{E+F}{2F}}\,\mathcal{K}\left(\dfrac{E+F}{2F}\right) & \text{for} \quad E < F \end{cases}$$

where $\mathcal{K}(\kappa)$ is the complete elliptic integral of the first kind.

A.2. Action–angle variables for the pendulum

The generating function for the transformation to action–angle variables reads

$$W(J,q) = \int_0^q \mathrm{d}q \sqrt{\frac{2(E(J) + F\cos q)}{G}}$$

which gives

$$\begin{aligned} \Theta &= \frac{\partial W}{\partial J} \\ &= \frac{\mathrm{F}_1\left(\frac{E+F}{2F}, \arcsin\sqrt{\frac{2F}{E+F}}\sin q/2\right)}{4\mathcal{K}\left(\frac{E+F}{2F}\right)} \end{aligned}$$

and

$$q = 2\arcsin\left(\sqrt{\frac{E+F}{2F}}\,\mathrm{sn}\left(4\mathcal{K}\left(\frac{E+F}{2F}\Theta\right)\right)\right).$$

A.3. A short outline on elliptic integrals

Many different conventions for the elliptic integrals exist. The convention for elliptic integrals used in this paper follows those of Mathematica [26]. Thus

$$\begin{aligned} \mathrm{F}_1(\phi,\kappa) &= \int_0^{\phi} \frac{\mathrm{d}\theta}{\sqrt{1-\kappa\sin^2\theta}} \\ &= \int_0^{\sin\phi} \frac{\mathrm{d}t}{\sqrt{(1-t^2)(1-\kappa t^2)}} \end{aligned} \tag{A1}$$

$$\begin{aligned} \mathcal{K}(\kappa) &= \int_0^{\frac{\pi}{2}} \frac{\mathrm{d}\theta}{\sqrt{1-\kappa\sin^2\theta}} \\ &= \int_0^{1} \frac{\mathrm{d}t}{\sqrt{(1-t^2)(1-\kappa t^2)}} \end{aligned} \tag{A2}$$

$$\begin{aligned} \mathcal{E}(\phi,\kappa) &= \int_0^{\phi} \mathrm{d}\theta\,\sqrt{1-\kappa\sin^2\theta} \\ &= \int_0^{\sin\phi} \mathrm{d}t \sqrt{\frac{(1-\kappa t^2)}{(1-t^2)}} \end{aligned} \tag{A3}$$

$$\begin{aligned} \mathcal{E}(\kappa) &= \int_0^{\frac{\pi}{2}} \mathrm{d}\theta\,\sqrt{1-\kappa\sin^2\theta} \\ &= \int_0^{1} \mathrm{d}t \sqrt{\frac{(1-\kappa t^2)}{(1-t^2)}} \end{aligned} \tag{A4}$$

$$\Pi(n;\phi,\kappa) = \int_0^{\phi} \mathrm{d}\theta\,\frac{1}{(1-n\sin^2\theta)\sqrt{1-\kappa\sin^2\theta}} \tag{A5}$$

where $\mathrm{F}_1(\phi,\kappa)$, $\mathcal{K}(\phi,\kappa)$ and $\Pi(n;\phi,\kappa)$ are the elliptic integral of the first, second and third type. The complete elliptic integrals of the first and second type, $\mathcal{K}(\kappa)$ and $\mathcal{E}(\kappa)$, are defined for $m < 1$.

A.4. Various Fourier expansions

The derivation of the following Fourier series is given in [24]:

$$\mathrm{sn}(u,\kappa) = \frac{\pi}{\kappa\mathcal{K}(\kappa)} \sum \frac{\sin(2m-1)\frac{1}{2}\pi u/\mathcal{K}(\kappa)}{\sinh(2m-1)\frac{1}{2}\pi\mathcal{K}(\kappa')/\mathcal{K}(\kappa)} \tag{A6}$$

$$\mathrm{cn}(u,\kappa) = \frac{\pi}{\kappa K} \sum \frac{\cos(2m-1)\frac{1}{2}\pi u/\mathcal{K}(\kappa)}{\cosh(2m-1)\frac{1}{2}\pi\mathcal{K}(\kappa')/\mathcal{K}(\kappa)} \tag{A7}$$

$$\mathrm{dn}(u,\kappa) = \frac{\pi}{2\mathcal{K}(\kappa)} + \frac{\pi}{\mathcal{K}(\kappa)} \sum \frac{\cos m\pi u/\mathcal{K}(\kappa)}{\cosh m\pi\mathcal{K}(\kappa')/\mathcal{K}(\kappa)} \tag{A8}$$

$$\mathrm{am}(u) = \frac{\pi u}{2\mathcal{K}(\kappa)} + \sum \frac{\sin m\pi u/\mathcal{K}(\kappa)}{m\cosh m\pi\mathcal{K}(\kappa')/\mathcal{K}(\kappa)} \tag{A9}$$

$$\mathrm{sn}^2(u,\kappa) = \frac{1}{\kappa}\left(1 - \frac{\mathcal{E}(\kappa)}{\mathcal{K}(\kappa)} - \frac{\pi^2}{\mathcal{K}^2(\kappa)} \sum_{m=1}^{\infty} \frac{m\cos\left(\frac{m\pi u}{\mathcal{K}(\kappa)}\right)}{\sinh\left(\frac{m\pi\mathcal{K}(\kappa')}{\mathcal{K}(\kappa)}\right)}\right). \tag{A10}$$

References

[1] Bohr A and Mottelson B R 1975 *Nuclear Structure* vol 2 (New York: Benjamin)
[2] Heiss W D and Nazmitdinov R G 1994 *Phys. Rev. Lett.* **73** 1235
[3] Brack M and Bhaduri R K 1997 *Semiclassical Physics* (New York: Addison-Wesley)
[4] Heiss W D, Nazmitdinov R G and Radu S 1995 *Phys. Rev.* C **52** 3032
[5] Heiss W D and Nazmitdinov R G 1998 *Physica* D **118** 134
[6] Heiss W D, Lynch R A and Nazmitdinov R G 1999 *Phys. Rev.* C **60** 34 303
[7] Tomsovic S, Grinberg M and Ulmo D 1995 *Phys. Rev. Lett.* **75** 4346
Ulmo D, Grinberg M and Tomsovic S 1996 *Phys. Rev.* E **54** 136
[8] Main J and Günter W 1999 *Phys. Rev. Lett.* **82** 3038
[9] Gutzwiller M C 1990 *Chaos in Classical and Quantum Mechanics* (New York: Springer)
[10] Carnegie A and Percival I 1984 *J. Phys. A: Math. Gen.* **17** 801
[11] Dorizzi B, Grammaticos B and Ramani A 1983 *J. Math. Phys.* **24** 2282
[12] Dahlqvist P and Russberg G 1990 *Phys. Rev. Lett.* **65** 2837
[13] Eckhardt B, Hose G and Pollak E 1989 *Phys. Rev.* A **39** 3776
[14] Eckhardt B 1988 *Phys. Rep.* **163** 205
[15] Zakrzewski J and Marcinek R 1990 *Phys. Rev.* A **42** 7172
[16] Bohigas O, Tomsovic S and Ullmo D 1993 *Phys. Rep.* **223** 43
[17] Kotzé A A 1992 *PhD Thesis* University of the Witwatersrand, Johannesburg
[18] Steeb W H, Louw J A, de Beer W and Kotzé A A 1988 *Phys. Scr.* **37** 328
[19] Mao J M and Delos JB 1992 *Phys. Rev.* A **45** 1746
[20] Peters A D, Jaffé C, Gao J and Delos J B 1997 *Phys. Rev.* A **56** 345
[21] Lichtenberg A J and Lieberman M A 1983 *Regular and Stochastic Motion* (New York: Springer)
[22] Baker J L and Gollub J P 1990 *Chaotic Dynamics—An Introduction* (Cambridge: Cambridge University Press)
[23] Goldstein H 1980 *Classical Mechanics* 2nd edn (New York: Addison-Wesley)
[24] Greenhill A G 1959 *The Application of Elliptic Functions* (New York: Dover)
[25] Chandre C, Govin M and Jauslin H R 1998 *Phys. Rev.* E **57** 1536
[26] Wolfram S 1995 *Mathematica: A System for Doing Mathematics by Computer* 3rd edn (Reading, MA: Addison-Wesley)